IOP Publishing Plasma Physics and Controlled Fusion
Plasma Phys. Control. Fusion **62** (2020) 045017 (9pp) https://doi.org/10.1088/1361-6587/ab74e6

Simulations of electromagnetic emission from colliding laser wakefields

I V Timofeev[1], E A Berendeev[2], V V Annenkov[1,3] and E P Volchok[1]

[1] Budker Institute of Nuclear Physics SB RAS, 630090, Novosibirsk, Russia
[2] Institute of Computational Mathematics and Mathematical Geophysics, 630090, Novosibirsk, Russia
[3] Novosibirsk State University, 630090, Novosibirsk, Russia

E-mail: timofeev@ngs.ru

Received 8 October 2019, revised 18 December 2019
Accepted for publication 11 February 2020
Published 26 February 2020

Abstract

Electromagnetic emission at the second harmonic of the plasma frequency produced by nonlinear interaction of counterpropagating laser-driven potential plasma waves are studied using particle-in-cell simulations. This process has been recently proposed as a method for generating high-power tunable THz radiation with a narrow spectral line-width (Timofeev *et al* 2017 *Phys. Plasmas* **24** 103106). In the present paper, we find the optimal conditions for demonstrating this phenomenon in a laboratory experiment that implies excitation of colliding wakefields by axially symmetric 830 nm Gaussian laser pulses with the total energy 0.2 J in a supersonic gas jet. It is shown that the emission mechanism based on the collision of different-size wakes is always accompanied with the mechanism of plasma antenna which begins to radiate electromagnetic waves after the build-up of periodic ion density modulation. Such additional emission makes hydrogen more attractive for this generating scheme than gases with heavier atoms.

Keywords: plasma wakefields, terahertz generation, electromagnetic emission at plasma frequency harmonics

(Some figures may appear in colour only in the online journal)

1. Introduction

Generation of electromagnetic (EM) radiation at harmonics of the plasma frequency ω_p via nonlinear interaction of electrostatic (potential) plasma waves is a fundamental problem which has long been studied in relation to both space and laboratory plasmas [1–5]. These emission processes are presently believed to play the role in solar radio-bursts [6–8] and laboratory experiments on terahertz generation in mirror traps [9–14] where potential plasma waves are excited by the directed electron flows. The same nonlinear processes may also generate EM radiation with much shorter wavelengths (UV and x-ray) in a solid-state plasma with counter-streaming electron fluxes arising during two-sided irradiation of a thin foil by relativistically strong laser pulses [15].

Much effort in recent years has been made for the development of high-power terahertz schemes based on various plasma processes capable of converting potential plasma waves in electromagnetic ones [16–19]. The attractive feature of plasma-based THz sources is a possibility to tune the emission frequency by varying the plasma density and to reach high values of emission power by exciting large-amplitude electric fields overcoming the threshold of matter destruction. For the linear transformation of subluminal potential plasma waves driven by laser or particle beams to superluminal electromagnetic modes, one should use either inhomogeneities of plasma density (regular [20] or periodic [16, 21]) or external magnetic fields [22–24]. Another opportunity to transfer electrostatic energy to EM oscillations is the nonlinear interaction of two potential plasma waves producing EM emission at the second harmonic of the plasma frequency. In contrast to ω_p-radiation generated at the plasma cut-off for EM waves, the second harmonic emission is not screened by the surrounding plasma and freely escapes from it. Since such a process can occur in a plasma with the uniform density, the produced radiation allows for a narrow spectral line-width. The possibility of efficient EM emission at $2\omega_p$ has been firstly found in a plasma with counter-streaming electron beams due to

three-wave interactions between dominant waves colliding at some acute angle [25–28]. In our recent papers [29, 30], we have shown that the similar EM emission process can also be efficiently realized via the head-on collision of Langmuir waves with differing potential profiles. The role of such colliding waves can be played by either plasma wakefields driven by femtosecond laser pulses focused in different-size spots [29] or unstable plasma oscillations excited by different-size electron beams via the two-stream instability [30].

The main advantage of the scheme with colliding wakefields is the possibility to generate GW, multi-mJ terahertz pulses by using modern petawatt-class laser systems [29]. Before reaching these record parameters at the most powerful facilities, we propose to verify the idea in a proof-of-principle experiment that is planned to be carried out using the terawatt laser system (830 nm, 0.2 J, $>$ 20 fs) developed in the Institute of Laser Physics (ILP SB RAS, Novosibirsk, Russia) [31]. In this experiment, by the collision of axially symmetric Gaussian laser pulses in a supersonic gas jet, we expect to demonstrate down-conversion of high-frequency laser radiation ($\lambda_0 = 830$ nm) to low-frequency THz radiation ($\lambda = 10\,\mu$m) with the efficiency exceeding 0.01%. The choice in favor of 10 μm (the wavelength of CO_2 laser) is made for more convenient detection of such radiation. The main goal of this experiment is to prove the principal possibility of such down-conversion which can be easily scaled to high-power CO_2 laser drivers capable of producing much lower THz frequencies. Thus, the goal of the present paper is to find the optimal parameters for this demonstration experiment and confirm the performance of the proposed generating scheme in the optimal regime by full-scale particle-in-cell (PIC) simulations. Feasibility of the scheme with colliding laser pulses at high intensities has been already demonstrated experimentally [32] with regard to the problem of electrons injection in a wakefield accelerator.

Our simulations of the discussed phenomenon reveal that the collision of plasma wakes with differing potential profiles is not the only mechanism that contribute to radial EM emission at the second harmonic of the plasma frequency. The comparable contribution to the total energy of the produced radiation comes from the mechanism of plasma antenna [33–36] which begins to work after modulation of ion density by oppositely moving wakes. The period of this modulation is too short to generate ω_p-radiation via the linear conversion of each wake [21], but is appropriate for nonlinear interaction of the primary wake with its long-wavelength satellite reflected from the ion density perturbation [37]. Due to formation of an inhomogeneous ion density with the well predictable spatial structure, the proposed experiment will allow us to study the mechanism of the second harmonic antenna emission in that simplified form which is usually discussed in idealized theoretical models and will give us important information for understanding similar emission processes occurring in more complex unstable electron beam-plasma systems.

2. Radiation mechanisms

Let us calculate the power of the second harmonic emission produced by colliding plasma wakefields. Superposition of two Langmuir waves (wakes) driven by the ponderomotive forces of counterpropagating short laser pulses with relatively small strength parameters ($a^2 \ll 1$) and equal wavelengths can be described by the electrostatic potential

$$\Phi(\mathbf{r}, t) = \Phi_1(\mathbf{r}_\perp)e^{ikz-i\omega t} + \Phi_2(\mathbf{r}_\perp)e^{-ikz-i\omega t} + \text{c.c.} \qquad (1)$$

All perturbations associated with excited plasma waves should oscillate with the plasma frequency $\omega_p = \sqrt{4\pi e^2 n_0/m_e}$ (n_0 is the unperturbed electron plasma density, e and m_e are the charge and mass of an electron) and move in opposite z-directions with the phase velocities equal to the laser group velocity ($\omega/k = v_g$). Further we will use dimensionless units, where time is measured in ω_p^{-1}, spatial coordinates in c/ω_p, velocities in the speed of light c, frequencies in ω_p, wavenumbers in ω_p/c, potentials Φ in $m_e c^2/e$, EM fields in $em_e c/\omega_p$, electric currents in $e\,n_0 c$. In such units, the frequency and parallel wavenumber of each wake are equal to $\omega = 1$ and $k = 1/v_g = 1/\sqrt{1 - 1/\omega_0^2}$ where ω_0 is the laser frequency. In a homogeneous isotropic plasma, these subluminal waves cannot get in resonance with electromagnetic modes. EM radiation can be generated by either nonlinear interaction of these potential waves or their conversion on ion density gradients.

In an overlapping region, one wave can be scattered by electron density perturbations created by a counter-propagating wave even in the case of uniform ion density. Such nonlinear interaction generates the longitudinal electric current

$$j_z(\mathbf{r}, t) = \mathcal{J}(\mathbf{r}_\perp)e^{-2i\omega t} + \text{c.c.}, \qquad (2)$$

$$\mathcal{J}(\mathbf{r}_\perp) = -\frac{1}{4}(\delta n_1 v_{2z} + \delta n_2 v_{1z}), \qquad (3)$$

which is able to radiate electromagnetic waves at the second harmonic of the plasma frequency transversely to the propagation axis. In the linear approximation, amplitudes of density and velocity perturbations for plasma electrons take the form:

$$v_{1z} = -k\Phi_1(\mathbf{r}_\perp), \quad v_{2z} = k\Phi_2(\mathbf{r}_\perp), \qquad (4)$$

$$\delta n_{1,2} = (\Delta_\perp - k^2)\Phi_{1,2}(\mathbf{r}_\perp), \qquad (5)$$

where $\Delta_\perp = \nabla_\perp \cdot \nabla_\perp$ is the transverse part of the Laplace operator. Substituting these formulas in equation (3), we obtain the amplitude of the radiating current

$$\mathcal{J}(\mathbf{r}_\perp) = \frac{k}{4}(\Phi_1\Delta_\perp\Phi_2 - \Phi_2\Delta_\perp\Phi_1). \qquad (6)$$

It is seen that this current disappears not only for plane waves (when $\Phi_{1,2}$ do not depend on $\mathbf{r}_\perp$), but also for waves with locally equal transverse profiles ($\Phi_1(\mathbf{r}_\perp) = \Phi_2(\mathbf{r}_\perp)$). In order to produce radiation in such a scheme, potential plasma waves should either have different transverse structures or collide with a finite impact parameter.

Let us consider generation of EM radiation by the nonlinear current (3) in the case of axially symmetric Gaussian laser pulses propagating along the same axis. The amplitude

of electric field $E_z = \mathcal{E}(r)e^{-2i\omega t} + \text{c.c.}$ in the produced EM wave inside the plasma can be found from the Maxwell equations which in the axially symmetric case are reduced to the following simple form:

$$\left[\frac{1}{r}\frac{\partial}{\partial r}r\frac{\partial}{\partial r} + 3\right]\mathcal{E}(r) = -2i\mathcal{J}(r). \tag{7}$$

By matching the solution of this equation at the plasma boundary $r = R$ with a radially convergent EM wave in vacuum $E_z = (C/\sqrt{r})e^{2ir-2it} + \text{c.c.}$, we find the maximal amplitude of the EM wave escaping from the plasma:

$$\mathcal{E}_0 = \left|\frac{2C}{\sqrt{R}}\right| = \frac{2}{\sqrt{(2\sqrt{3}RJ_1 - J_0)^2 + 16R^2J_0^2}} \times \left|\int_0^R rJ_0(\sqrt{3}r)\mathcal{J}(r)dr\right|, \tag{8}$$

where J_0 and J_1 are the Bessel functions of the argument $\sqrt{3}R$. Calculating the normal component of the Poynting flux penetrating through the plasma boundary, we obtain the total power radiated from the whole plasma column at the second harmonic of the plasma frequency

$$\mathcal{P} = \frac{P}{P_0} = \pi R\int\mathcal{E}_0^2 dz, \quad P_0 = \frac{m_e c^5}{4\pi e^2} \approx 0.69\text{GW}. \tag{9}$$

Here, we take into account the slow ($|\partial/\partial z| \ll k, |\nabla_\perp|$) dependence of radiation wave amplitude on the longitudinal coordinate z caused by diffraction of laser drivers.

If envelopes of linearly polarized laser pulses focused into the planes $z = z_s$ with the spot-sizes σ_{0s} are described by the normalized vector potentials

$$a_s = a_{0s}\frac{\sigma_{0s}}{\sigma_s(z)}e^{-r^2/\sigma_s^2(z)}\sin^2\left(\frac{\pi(t \pm z)}{2\tau}\right), \tag{10}$$

$$\sigma_s(z) = \sigma_{0s}\sqrt{1 + (z - z_s)^2/\mathcal{R}_s^2}, \quad \mathcal{R}_s = \omega_0\sigma_{0s}^2/2, \tag{11}$$

amplitudes of excited plasma wakes take the form:

$$\Phi_s(r) = \Phi_s^w\left(\frac{\sigma_{0s}}{\sigma_s(z)}\right)^2 e^{-2r^2/\sigma_s^2(z)}, \tag{12}$$

$$\Phi_s^w = \frac{3}{4}a_{0s}^2\frac{\sin\tau}{4 - 5\tau^2/\pi^2 + \tau^4/\pi^4}. \tag{13}$$

Substituting these formulas in equations (6) and (8) and assuming that the plasma radius is markedly greater than the laser waist-sizes, we can extend integration in (8) to infinite limits and derive the following analytic expression for the radiation wave amplitude:

$$\mathcal{E}_0 = \frac{3\Phi_1^w\Phi_2^w\mathcal{F}_\sigma}{2\sqrt{(2\sqrt{3}RJ_1 - J_0)^2 + 16R^2J_0^2}}, \tag{14}$$

$$\mathcal{F}_\sigma = \frac{\sigma_{01}^2\sigma_{02}^2|\sigma_2^2 - \sigma_1^2|}{(\sigma_1^2 + \sigma_2^2)^2}\exp\left[-\frac{3}{8}\frac{\sigma_1^2\sigma_2^2}{\sigma_1^2 + \sigma_2^2}\right]. \tag{15}$$

By analyzing the factor $\mathcal{F}_\sigma$, one can find optimal conditions for spatial overlapping of colliding plasma wakefields.

Standing plasma oscillations formed by counter-propagating wakes in the overlapping region create the ponderomotive force on electrons pushing them out of wave antinodes. It results in rapid ion density modulation with the wavenumber $q = 2k$ via the arising space charge electric field. On the one hand, such a density modulation destroys plasma oscillations and shortens their life-time, but on the other hand it switches on an additional radiation mechanism referred to as the plasma antenna [33, 34]. The essence of the mechanism is excitation of superluminal forced plasma oscillations due to scattering of a primary subluminal potential wave on a quasi-stationary ion density perturbation. If the produced plasma channel is comparable in sizes with the radiation wavelength, these fast oscillations are capable of radiating obliquely propagating vacuum EM waves. In the case of laser drivers, the fundamental emission ($\omega = 1$) can be produced via the linear process $(\omega, k) + (0, -q) \to (\omega, k - q)$ [21] if the modulation wavenumber falls in the range $1 - v_g < q/k < 1 + v_g$. In our case $q = 2k$, the modulation period appears to be too short to produce oscillations moving faster than light, but it is appropriate for generating the second harmonic radiation by the nonlinear process $(\omega, k) + (\omega, k - q) \to (2\omega, 2k - q)$ [37]. Indeed, resulting oscillations $(2\omega, 2k - q)$ become superluminal inside a wider range of q $(1 - v_g < q/(2k) < 1 + v_g)$. The middle of this range corresponds to emission in the purely transverse direction [21].

Thus, EM waves at the second harmonic of the plasma frequency radiated transversely to the axis of wakes collision can be generated by two different mechanisms: the first one is based on the nonlinear interaction of primary laser-driven wakes with mismatching potential profiles in a uniform density plasma, and the second one suggests the same interaction, but the role of counterpropagating wave is played here by a satellite of a primary wave scattered by the ion density perturbation.

3. Optimal parameters for demonstration experiment

Let us find out the optimal overlapping scheme for colliding plasma wakes which maximizes the radiation efficiency η. We define this quantity as the fraction of laser energy that is converted to electromagnetic radiation at the second harmonic of the plasma frequency ($\eta = \mathcal{W}_R/\mathcal{W}_L$). Assuming that the characteristic duration of the produced radiation τ_R in our axially symmetric problem remains the same as in recent 2D3V PIC simulations in Cartesian geometry [29] ($\tau_R \simeq 100$) and does not significantly depend on spot-sizes of laser beams, the energy of the low-frequency radiation pulse can be estimated as $\mathcal{W}_R = \int\mathcal{P}dt \simeq \mathcal{P}\tau_R$ (in units of P_0/ω_p). In our previous paper [29], we searched for the optimal overlapping of laser-driven wakefields in the case when the colliding laser pulses had equal energies, were focused into rectangular spots stretched in one direction and were limited in waist amplitudes by the validity of electrostatic approximation for excited wakes ($a_{0s} \leqslant 0.7$). Here, we should find similar optimal conditions for the collision of axially symmetric Gaussian laser pulses with the given total energy 0.2 J and wavelength $\lambda_0 = 830$ nm which are typically produced by the terawatt

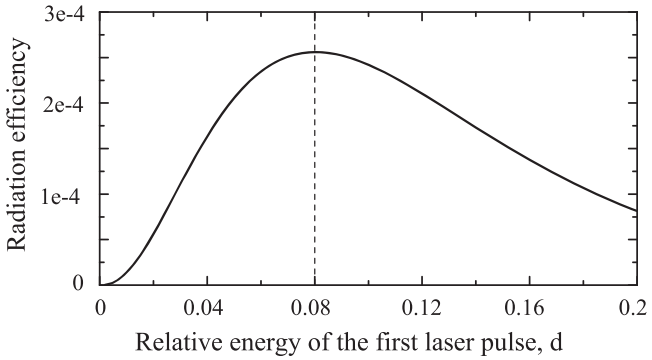

Figure 1. The radiation efficiency η as a function of the relative energy content of the first laser pulse $d = \mathcal{W}_{L1}/\mathcal{W}_L$ in the case $a_{01} = a_{02} = 0.7$.

laser system developed in the Institute of Laser Physics (ILP SB RAS, Novosibirsk). Since laser pulses are planed to be collided in a finite-size (∼1 mm) supersonic gas jet in a future experiment, it is more preferable to use the most compact overlapping scheme as to avoid the influence of density inhomogeneity on the line-width of produced radiation. The most compact radiating zone along the optical axis is realized for the scheme with the matched focal planes ($z_1 = z_2 = 0$) and different spot-sizes ($\sigma_{01} \neq \sigma_{02}$). It is obvious that the symmetric distribution of energy between colliding laser pulses discussed in [29] is not the optimal one for such a scheme if laser amplitudes are limited by the validity of electrostatic approximation for excited wakes ($a_{0s} \leqslant 0.7$). Indeed, different-size laser pulses with equal energies

$$\mathcal{W}_{L1} = \frac{3\pi}{16}\tau\omega_0^2 a_{01}^2\sigma_{01}^2 = \frac{3\pi}{16}\tau\omega_0^2 a_{02}^2\sigma_{02}^2 = \mathcal{W}_{L2} \qquad (16)$$

should also have different amplitudes (for example, if we chose $a_{01} = 0.7$ for the narrow beam, we need a lower amplitude $a_{02} = a_{01}\,\sigma_{01}/\sigma_{02} < a_{01}$ for the wide beam). Due to the strong dependence of radiation power on laser amplitudes $\mathcal{P} \propto a_{01}^4 a_{02}^4$, it is more efficient to use equal maximal values of the normalized vector potential ($a_{01} = a_{02} = 0.7$). Calculating the radiation efficiency from the theory presented in section 2, one can find the optimal relative energies $\mathcal{W}_{L1}/\mathcal{W}_L = d$ and $\mathcal{W}_{L2}/\mathcal{W}_L = 1 - d$ that should be contained in colliding pulses.

To demostrate generation of EM radiation at the frequency $2\omega_p/(2\pi) = 28.4$ THz, laser pulses should create a plasma channel with the electron density $n_0 = 2.5 \times 10^{18}\,\mathrm{cm}^{-3}$. Such a density is much lower than the critical density for laser radiation ($\omega_0 = 25.4$). The maximal amplitude of a plasma wake (13) is achieved if the duration of a laser driver equals approximately to a half-period of plasma oscillations $\tau = 3.48$ (in dimensional units $\tau = 39$ fs). For these parameters, the dependence of radiation efficiency on the relative energy content of the first laser pulse $\eta(d)$ is presented in figure 1.

It is seen that the most efficient generation of THz radiation is achieved when 8% of the total laser energy falls on the first pulse with the narrow focal spot $\sigma_{01} = 1.78$ and 92% is contained in the wide laser pulse with $\sigma_{02} = 6.03$.

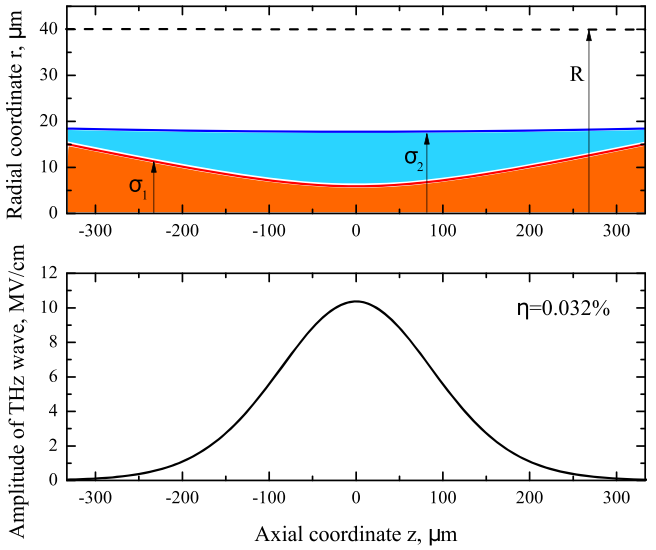

Figure 2. Optimal spatial overlapping of colliding plasma wakes (a) and the amplitude of the radiated THz wave $\mathcal{E}_0$ (b) calculated from equation (14) for the parameters of demonstration experiment (table 1).

Unfortunately, our assumption about independence of τ_R on laser spot-sizes is not valid for strongly nonlinear wakes with the typical life-time shorter than $\tau_R \simeq 100$. As an indicator of plasma wave nonlinearity, we will consider the electron density perturbation $\delta n_s = \Phi_s^w(1 + 8/\sigma_{0s}^2)$. At small laser waist-sizes, plasma waves become strongly nonlinear $\delta n \sim 1$ even for the moderate values of laser fields $a_{01} = a_{02} = 0.7$. In the optimal regime discussed above, density perturbations excited independently by laser pulses reach the values $\delta n_1 = 0.68$ and $\delta n_2 = 0.23$. Our PIC simulations show that these two wakes should have sufficiently differing wavebreaking times [38] which is not optimal for the collision scheme. To reduce this difference, we slightly decrease the amplitude of the narrow pulse ($a_{01} = 0.67$) and increase the amplitude of the wide pulse ($a_{02} = 0.8$). For the same energy distribution between colliding pulses, it corresponds to the spot-sizes $\sigma_{01} = 1.86$, $\sigma_{02} = 5.28$ and density perturbations $\delta n_1 = 0.58$, $\delta n_2 = 0.33$. The validity of the electrostatic theory for excitation of plasma wakes at these parameters is further verified using special PIC simulations.

In hydrogen, the plasma radius should be determined by the barrier-suppressed ionization produced by the electric field of the second laser pulse. We can neglect diffraction spreading of this pulse along the length of radiating region and estimate the radius of ionized plasma channel as $R = 12$. The spatial arrangement of laser tricks and corresponding amplitude profile of the produced EM wave at the plasma boundary are shown in figure 2.

For the selected parameters of the future experiment gathered in the dimensional form in table 1, our theory predicts that the total power and energy of the produced pulse of the second harmonic radiation with the typical duration 1 ps should reach 57 MW and 57 μJ, respectively. It corresponds to the efficiency of laser-to-THz energy conversion $\eta =$ 0.032%.

Table 1. Parameters of demonstration experiment.

Parameter	Value
Laser wavelength, λ_0	830 nm
Energy of the 1st laser pulse, $\mathcal{W}_{L1}$	16 mJ
Energy of the 2st laser pulse, $\mathcal{W}_{L2}$	184 mJ
Spot-size of the 1st laser pulse, σ_{01}	6.3 μm
Spot-size of the 2st laser pulse, σ_{02}	18 μm
Maximal laser strength, a_{01}	0.67
Maximal laser strength, a_{02}	0.8
Duration of laser pulses, τ	39 fs
Density of plasma electrons, n_0	$2.5 \cdot 10^{18}$ cm^{-3}
Radius of plasma channel, R	40 μm
Length of radiating plasma channel	0.6 mm
Nozzle diameter	1.5 mm
Frequency of THz radiation, $2\omega_p/(2\pi)$	28.4 THz

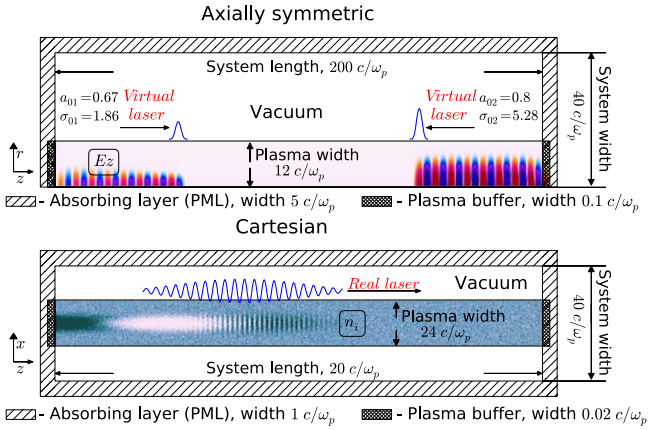

Figure 3. The layout of the simulation box in axially symmetric (top) and Cartesian (bottom) geometry.

It should be remembered, however, that the analytical theory used here to find the optimal regime of EM emission is able to predict the maximal radiation intensity achieved in different points along the optical axis, but cannot predict the pulse duration which is strongly affected by other complicated nonlinear processes resulting in dissipation of wakes energy. Our estimate $\tau_R \simeq 100$ is based on recent PIC simulations [29] which were carried out in slab geometry and did not account for ion dynamics. Thus, to estimate the performance of the proposed generating scheme for selected parameters of the future laboratory experiment, we need to carry out PIC simulations in the more realistic axially symmetric case and study effects of mobile plasma ions.

4. PIC model

To study EM emission produced by colliding plasma wakes, we use two different numerical models based on the PIC method. The first 2D3V model is used to simulate the process in axially symmetric (r, z) geometry. Such a model is not suitable for studying self-consistent dynamics of real laser fields, but allows to simulate the whole length of radiating plasma column using the approach of virtual laser pulses in which the action of laser fields on plasma electrons are described by the slow-varying ponderomotive force only ($\mathbf{F}_s = -\nabla|a_s(\mathbf{r}, t)|^2/4$). To verify the validity of this simplified approach for the discussed parameters, we use the second 2D3V model operating in Cartesian (x, z) geometry and allowing to simulate self-consistent evolution of real laser fields polarized transversely to the z-axis. Due to the need to resolve the laser wavelength in this model, our test simulations are limited by relatively small plasma lengths.

We use the well known algorithms of Boris and Yee to calculate evolution of particles and fields, and Esirkepov's scheme to calculate currents. The layout of our simulation box is shown in figure 3.

In the axially symmetric problem, we simulate a plasma column of radius $R = 12$ in which electrons and ions are uniformly distributed with equal densities. In slab geometry, we consider the infinite plasma layer with the transverse size $L_x = 2R = 24$. Electrons are characterized by the Maxwellian momentum distribution $f_e \propto \exp(-\mathbf{p}^2/(2\Delta p_e^2))$ with the temperature $T_e = \Delta p_e^2/(2m_e) = 14$ eV and ions are assumed to be cold. To study effects of ion dynamics, we use real ion masses for hydrogen and helium and, to separate the contribution of antenna emission, we perform simulations with immobile ions.

Simulation starts from the state of completely compensated electric charge and zero EM fields. Then we inject virtual laser pulses into the plasma by acting on plasma electrons through the additional ponderomotive forces $\mathbf{F}_s(\mathbf{r}, t)$ which are calculated for the given envelopes a_s (10) of diffracting laser pulses. Both colliding pulses are focused to the middle of the plasma column $z = 100$ and arrive to the focal plane at the same time. We use the same laser and plasma parameters as in table 1. In order to exclude parasitic transition radiation, ponderomotive forces of virtual laser pulses are smoothly reduced to zero while approaching plasma boundaries. Since there is no need to resolve the laser wavelength in the axially symmetric model, we use the large spatial grid $\Delta r = \Delta z = 0.05$ with the time step $\Delta t = 0.025$ and 144 macroparticles with the parabolic form-factor in a cell for each sort.

In slab geometry, we create the self-consistently evolving laser radiation by setting high-frequency ($\omega_0 = 25.4$) EM fields (E_y, B_x) with the given envelopes at simulation boundaries. Here, we use higher spatial and temporal resolution $\Delta x = \Delta z = 0.01$, $\Delta t = 0.005$ with 81 computational particles in a cell.

At the ends of plasma column, we use open boundary conditions supporting macroscopic plasma homogeneity near the boundaries. They are realized using special buffers creating incoming particles and removing outgoing ones. More detailed description of these conditions can be found in [30]. To prevent reflection of the generated EM radiation from the boundaries of the simulation box and further accumulation of its energy in a system, we use the perfectly matched layers [39]. The power of the produced radiation is calculated as the normal component of the Poynting flux averaged over the

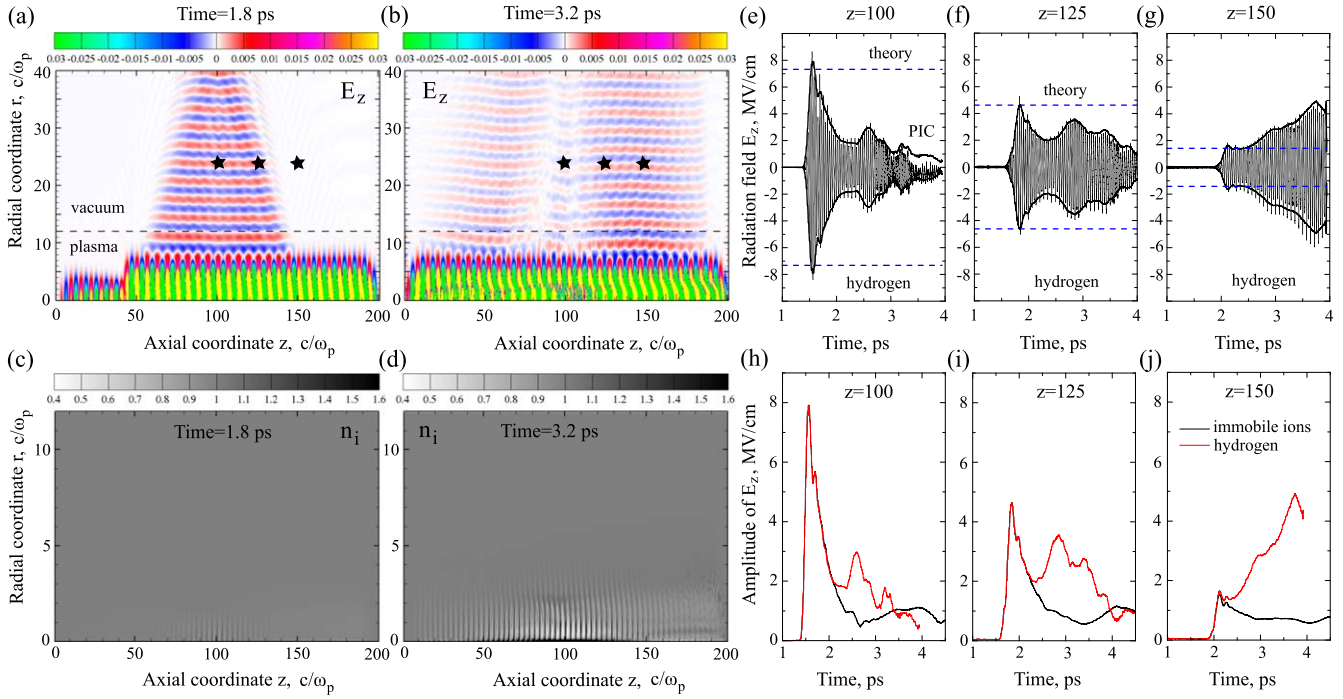

Figure 4. Results of PIC simulations: (a) the map of electric field $E_z(r, z)$ in the moment $t = 1.8$ ps for real-mass hydrogen ions (black stars show the points where we measure temporal evolution of radiation fields), (b) the map of electric field $E_z(r, z)$ in the moment $t = 3.2$ ps for real-mass hydrogen ions, (c) density of hydrogen ions $n_i(r, z)$ in the moment $t = 1.8$ ps, (d) density of hydrogen ions $n_i(r, z)$ in the moment $t = 3.2$ ps, (e)–(g) history of electric field E_z in different spatial points $z = 100$, 125, 150 indicated by black stars in case of real-mass hydrogen ions, (h)–(j) temporal dependence of radiation field amplitudes (envelopes of E_z oscillations) for real-mass hydrogen (red) and immobile (black) ions.

period of electromagnetic oscillations and integrated over the wall area.

5. Simulation results

Let us first carry out full-scale simulations of THz generation using virtual laser pulses and then verify the accuracy of this simplified approach to the description of nonlinear wakes participating in the collision process.

5.1. Collision of axially symmetric wakes

Results of PIC simulations in axially symmetric geometry are presented in figure 4. Here, we simulate the collision of different-size laser pulses with the parameters $a_{01} = 0.67$, $\sigma_{01} = 1.86$, $a_{02} = 0.8$, $\sigma_{01} = 5.28$ discussed in section 3. At the early stage $t = 1.8$ ps of wakes interaction (figures 4(a) and (c)) when the ion density of hydrogen plasma is not yet significantly perturbed, the observed EM emission is really produced via the collision of plasma wakes with mismatching potential profiles. It is seen that EM waves escaping from the plasma in the purely transverse direction are generated inside the region of wakes overlapping only (figure 4(a)) and the frequency of this radiation is concentrated near the second harmonic of the plasma frequency (figure 5).

Moreover, the amplitudes of the emitted waves in different spatial points along the optical axis are initially coincide with our theoretical predictions (figures 4(e)–(g)).

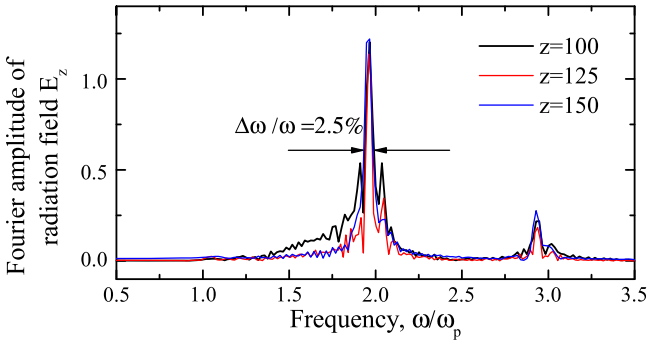

Figure 5. Frequency spectra of radiation fields E_z in different z-points.

Further temporal evolution of the radiation amplitude in these points, however, demonstrates the rapid decrease of the radiation electric field E_z near the focal plane and, in contrast, its significant growth in remote regions. The same effect is also visible from figure 4(b) presenting the map of electric field $E_z(r, z)$ in the later moment of time $t = 3.2$ ps. From the map of ion density $n_i(r, z)$ in the same moment shown in figure 4(d), we can conclude that THz generation at this stage must be strongly affected by the deep density modulation with the wavenumber $q = 2$ created by the ponderomotive force of standing plasma oscillations. This modulation results in dissipation of energy accumulated in plasma wakes, but can also switch on the additional radiation mechanism of plasma antenna allowing each wake to generate EM radiation

via scattering on the arising density perturbation. To demonstrate the influence of ion dynamics on the duration of the second harmonic emission, we perform simulations with immobile ions. Results of these simulations are compared with the results obtained for real-mass hydrogen ions in figures 4(h)–(j). It is seen that the rapid decrease of the radiation wave amplitude observed in hydrogen just after reaching the predicted maximal level (in spatial points $z = 100$ and $z = 125$) is also reproduced in the case of uniform ion density. It means that electron nonlinearities responsible for the energy transfer from primary wakes to non-radiating harmonics are the main reason for limiting the energy of a THz pulse produced by the mechanism of wakes collision. It is also seen that the duration of the most intense THz radiation generated in the focal spot (figure 4(h)) appears to be twice shorter than the expected value $\tau_R \simeq 100 \approx 1$ ps observed in earlier simulations in slab geometry and used in our theoretical estimates. At the later stage of wakes interaction ($t > 2.5$ ps), ion dynamics becomes important resulting in enhancement of EM radiation compared to the level of emission produced in the plasma with immobile ions (figures 4(h)–(j)). This enhancement is seen in all observation points and becomes more pronounced as moving away from the focal plane.

In our opinion, the presented simulations with mobile and immobile ions allow us to separate contributions of different radiation mechanisms to the total power of the second harmonic emission shown in figure 6(a). In the case of immobile (or infinite-mass) ions, EM emission is completely determined by the collision of counterpropagating wakes with different potential profiles, while in the case of mobile ions we observe additional EM emission produced by each wake via the mechanism of plasma antenna. Despite the fact that the maximal amplitude of the radiated EM wave in each spatial point along z-axis is correctly predicted by our theory, the total power emitted from the whole plasma volume turns out to be twice lower than the theoretical value calculated from equation (9) (figure 6(a)). It is explained by the short duration of the produced THz pulse which is actually shorter than the time required for the laser pulse to pass the half-length of radiating plasma. Thus, the maximal radiation amplitude is never simultaneously achieved over the whole radiating zone. By integrating the radiation power over time, we calculate what part of the laser energy is transformed to the energy of the second harmonic radiation (figure 6(b)). In gases with light atoms (hydrogen or helium), this radiation efficiency is seen to grow during 3 ps and be saturated at the level of 0.02%. Approximately a half of the total EM energy is radiated via the mechanism of wakes collision during the first picosecond and the remaining half is produced via the antenna mechanism. The presence of this additional radiation mechanism makes hydrogen more attractive for the proposed generating scheme compared to gases with heavier atoms.

Thus, full-scale simulations of the proposed demonstration experiment show that collision of laser-driven plasma wakes inside the ionized channel created in a supersonic gas jet is able to generate a narrow-band ($\Delta\omega/\omega = 2.5\%$) THz radiation pulse with the energy conversion efficiency exceeding $\eta = 0.02\%$.

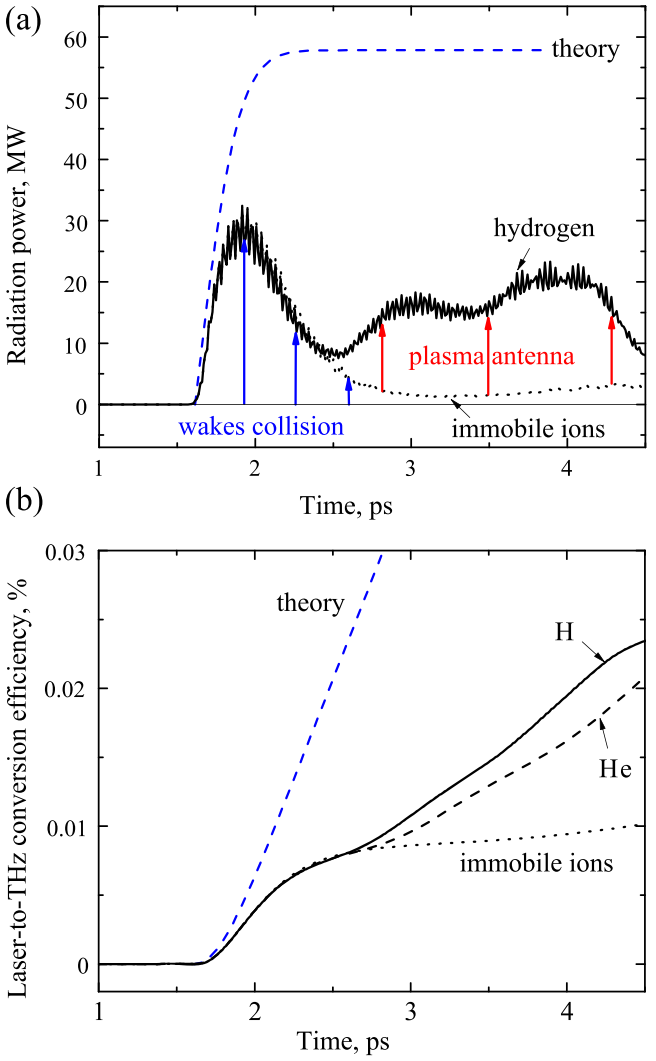

Figure 6. (a) The history of the total radiation power measured in PIC simulations for hydrogen ions (black solid) and immobile ions (black points). Theoretical prediction (9) for the uniform ion density is shown by the blue dashed curve. (b) Laser-to-THz energy conversion efficiency η as a function of time for hydrogen, helium and infinite-mass ions.

5.2. Excitation of wakes by real laser pulses

Let us now verify how accurately the approach of virtual laser pulses describes excitation of plasma wakefields for the discussed parameters. Such a simplified approach is valid only for relativistically weak laser fields ($a_0^2 \ll 1$) capable of driving almost electrostatic plasma waves via the potential ponderomotive force. The conventional boundary of applicability of such a relativistically weak regime can be set as $a_0 = 0.7$. In section 3, we have found reasonable to increase the waist amplitude of the wider laser pulse up to the value $a_0 = 0.8$ as to minimize the life-time difference for colliding wakes. Thus, we have to verify whether the amplitude of electrostatic potential of a single laser-driven wake is correctly predicted by equation (13) derived in the electrostatic limit.

We carry out 2D3V high-resolution PIC simulations in slab geometry to study excitation of each plasma wake participating in the collision process by its own self-consistently

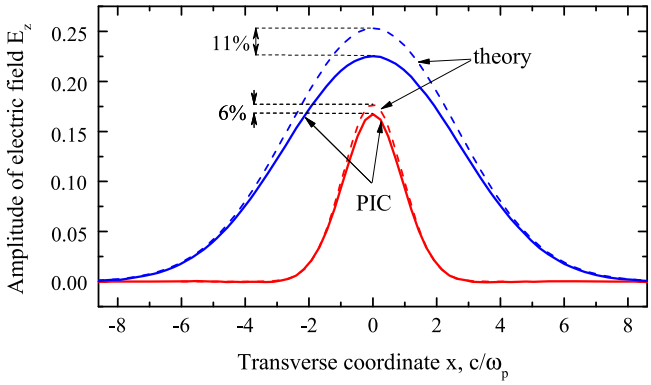

Figure 7. Transverse profiles of the maximal longitudinal electric field $E_z(x)$ in the wide and narrow wake observed in PIC simulations (solid) and predicted by the electrostatic theory (dashed).

evolving laser pulse. According to equation (13), maximal amplitudes of longitudinal electric field $E_z = |k\Phi_s(0)| = |\Phi_s^w|$ of the excited wakes in the focal plane should reach the values $\Phi_1^w = 0.177$ and $\Phi_2^w = 0.253$. Comparison of transverse profiles of wake amplitudes $\Phi_1(x)$ and $\Phi_2(x)$ predicted theoretically (12) with corresponding profiles of electric field E_z observed in PIC simulations is shown in figure 7.

It is seen that amplitudes of the narrow and wide plasma wake in PIC simulations are reduced compared to their theoretical predictions by 6% and 11%, respectively. Substituting the reduced profiles in equation (8), we find that the electric field amplitude $\mathcal{E}_0$ of EM wave emitted from the focal plane getting lower by 17%. Taking into account the scaling $\mathcal{P} \propto \mathcal{E}_0^2$ and less deviation from theory in regions distant from focus, we can expect that results of PIC simulations with virtual laser pulses shown in figure 6(b) overestimate the efficiency of laser-to-THz energy conversion by no more than 30%.

6. Conclusion

In this paper, we discuss optimal parameters for the laboratory experiment aimed at demonstration of the principal possibility to generate high-power narrow-band THz radiation via nonlinear interaction of counterpropagating laser-driven plasma wakes. Such a proof-of-principal experiment is planned to be set up in the Institute of Laser Physics in Novosibirsk (Russia) using the terawatt laser system capable of producing 830 nm laser pulses with the minimal duration 20 fs and total energy 0.2 J. Based on the analytical theory of the discussed phenomenon, we have found the optimal distribution of energy between colliding laser pulses and optimal conditions for their focusing providing the most efficient conversion of laser energy to EM radiation at the second harmonic of the plasma frequency (28 THz). Full-scale axially symmetric PIC simulations of EM emission from colliding plasma wakefields confirm theoretical predictions for maximal amplitudes of radiated EM waves achieved in different points along the optical axis, but demonstrate a considerable decrease in the duration of the produced EM pulse in comparison with the results of earlier PIC simulations in Cartesian slab geometry. It is shown that the mechanism of wakes collision in that form which is theoretically predicted for the uniform ion density works only during the first picosecond of wakes interaction. The duration of this emission stage is limited by electron nonlinearities resulting in the rapid transfer of energy from primary wakes to non-radiating harmonics. In a plasma with finite-mass ions, the mechanism based on the collision of plasma wakes with differing potential profiles is found to pass the baton to the mechanism of plasma antenna based on scattering of each wake by the longitudinal ion density modulation. The maximal contribution of this additional mechanism to the total radiation energy is achieved by using hydrogen as a working gas. The resulting THz pulse with the narrow line-width ($\Delta\omega/\omega \approx 2.5\%$) generated by both mechanisms is predicted to reach the maximal power 20–30 MW and total energy 30–40 μJ corresponding to the efficiency of optical-to-THz energy conversion 0.015%–0.02%.

The possibility of generating THz pulses with the power and energy exceeding typical parameters of free electron lasers by using more compact devices is interesting by itself, but the main goal of the proposed experiment is to verify our theoretical insights about the mechanisms of EM emission which can be easily scaled to the generation of GW, multi-mJ THz radiation by modern petawatt-class lasers. Since the head-on collision of potential plasma waves and their nonlinear conversion on periodic ion density perturbations are also responsible for EM emission in electron beam-plasma systems, experimental confirmation of these radiation mechanisms will be important for understanding EM wave generation in more complex phenomena in space and laboratory plasmas with colliding [40] and directed [8, 13] electron flows.

Acknowledgments

This work is supported by the Russian Scientific Foundation (grant 19-71-00054). Simulations are carried out using computational resources of Novosibirsk State University.

ORCID iDs

I V Timofeev https://orcid.org/0000-0001-5083-9777
V V Annenkov https://orcid.org/0000-0002-5577-8595

References

[1] Ginzburg V L and Zheleznyakov V V 1958 On the possible mechanisms of sporadic solar radio emission (radiation in an isotropic plasma) *Sov. Astron.* **2** 653
[2] Sturrock P A, Ball R H and Baldwin D E 1965 Radiation at the plasma frequency and its harmonic from a turbulent plasma *Phys. Fluids* **8** 1509

[3] Basov N G, Bychenkov V Yu, Krokhin O N, Osipov M V, Rupasov A A, Silin V P, Sklizkov G V, Starodub A N, Tikhonchuk V T and Shikanov A S 1979 Second harmonic generation in a laser plasma (review) *Sov. J. Quantum Electron.* **9** 1081

[4] Willes A J and Melrose D B 1997 The polarisation of second harmonic coronal type III bursts *Sol. Phys.* **171** 393

[5] Ziebell L F, Yoon P H, Petruzzellis L T, Gaelzer R and Pavan J 2015 Plasma emission by nonlinear electromagnetic processes *Astrophys. J.* **806** 237

[6] Ratcliffe H, Kontar E P and Reid H A S 2014 Large-scale simulations of solar type III radio bursts: flux density, drift rate, duration, and bandwidth *Astron. Astrophys.* **572** A111

[7] Thurgood J O and Tsiklauri D 2015 Self-consistent particle-in-cell simulations of fundamental and harmonic plasma radio emission mechanisms *Astron. Astrophys.* **584** A83

[8] Henri P, Sgattoni A, Briand C, Amiranoff F and Riconda C 2019 Electromagnetic simulations of solar radio emissions *J. Geophys. Res.: Space Phys.* **124** 1475

[9] Arzhannikov A V and Timofeev I V 2012 Generation of powerful terahertz emission in a beam-driven strong plasma turbulence *Plasma Phys. Control. Fusion* **54** 105004

[10] Burdakov A V *et al* 2013 Microwave generation during 100 keV electron beam relaxation in GOL-3 *Fusion Sci. Technol.* **63** 286

[11] Arzhannikov A V *et al* 2014 Observation of spectral composition and polarization of sub-terahertz emission from dense plasma during relativistic electron beam-plasma interaction *Phys. Plasmas* **21** 082106

[12] Ivanov I A *et al* 2015 MM-wave emission by magnetized plasma during sub-relativistic electron beam relaxation *Phys. Plasmas* **22** 122302

[13] Arzhannikov A V *et al* 2016 Dynamics and spectral composition of subterahertz emission from plasma column due to two-stream instability of strong relativistic electron beam *IEEE Trans. Terahertz Sci. Technol.* **6** 245

[14] Annenkov V V, Timofeev I V and Volchok E P 2019 Highly efficient electromagnetic emission during 100 keV electron beam relaxation in a thin magnetized plasma *Phys. Plasmas* **26** 063104

[15] Koester P *et al* 2015 Evidence of locally enhanced target heating due to instabilities of counter-streaming fast electron beams *Phys. Plasmas* **22** 020701

[16] Miao C, Palastro J P and Antonsen T M 2017 High-power tunable laser driven THz generation in corrugated plasma waveguides *Phys. Plasmas* **24** 043109

[17] Hur M S, Ersfeld B, Noble A, Suk H and Jaroszynski D A 2017 Increased impedance near cut-off in plasma-like media leading to emission of high-power, narrow-bandwidth radiation *Sci. Rep.* **7** 40034

[18] Kwon K B, Kang T, Song H S, Kim Y-K, Ersfeld B, Jaroszynski D A and Hur M S 2018 High-energy, short-duration bursts of coherent terahertz radiation from an embedded plasma dipole *Sci. Rep.* **8** 145

[19] Timofeev I V, Annenkov V V and Arzhannikov A V 2015 Regimes of enhanced electromagnetic emission in beam-plasma interactions *Phys. Plasmas* **22** 113109

[20] Sheng Z-M, Mima K, Zhang J and Sanuki H 2005 Emission of electromagnetic pulses from laser wakefields through linear mode conversion *Phys. Rev. Lett.* **94** 095003

[21] Volchok E P, Timofeev I V and Annenkov V V 2019 Coherent terahertz emission from a plasma layer due to linear conversion of laser wakefields on pre-modulated ion density *Plasma Phys. Control. Fusion* **61** 125006

[22] Yugami N, Higashiguchi T, Gao H, Sakai S, Takahashi K, Ito H, Nishida Y and Katsouleas T 2002 Experimental observation of radiation from Cherenkov wakes in a magnetized plasma *Phys. Rev. Lett.* **89** 065003

[23] Wang W-M, Gibbon P, Sheng Z M and Li Y T 2015 Tunable circularly polarized terahertz radiation from magnetized gas plasma *Phys. Rev. Lett.* **114** 253901

[24] Cho M-H, Kim Y-K, Suk H, Ersfeld B, Jaroszynski D A and Hur M S 2015 Strong terahertz emission from electromagnetic diffusion near cutoff in plasma *New J. Phys.* **17** 043045

[25] Intrator T, Hershkowitz N and Chan C 1984 Experimental observations of nonlinearly enhanced $2\omega_{UH}$ electromagnetic radiation excited by steady-state colliding electron beams *Phys. Fluids* **27** 527

[26] Schumacher R W, Santoru J, Rosenberg M and Krall N A 1993 Microwave/millimeter-wave generation in a counterstreaming-beam-plasma system *J. Appl. Phys.* **74** 3057

[27] Ganse U, Kilian P, Spanier F and Vainio R 2012 Nonlinear wave interactions as emission process of type II radiao bursts *Astrophys. J.* **751** 145

[28] Timofeev I V and Annenkov V V 2014 Efficient regime of electromagnetic emission in a plasma with counterstreaming electron beams *Phys. Plasmas* **21** 083109

[29] Timofeev I V, Annenkov V V and Volchok E P 2017 Generation of high-field narrowband terahertz radiation by counterpropagating plasma wakefields *Phys. Plasmas* **24** 103106

[30] Annenkov V V, Berendeev E A, Timofeev I V and Volchok E P 2018 High-power terahertz emission from a plasma penetrated by counterstreaming different-size electron beams *Phys. Plasmas* **25** 113110

[31] Bagayev S N, Leshchenko V E, Trunov V I, Pestryakov E V and Frolov S A 2014 Coherent combining of femtosecond pulses parametrically amplified in BBO crystals *Opt. Lett.* **39** 1517

[32] Faure J, Rechatin C, Norlin A, Lifschitz A, Glinec Y and Malka V 2006 Controlled injection and acceleration of electrons in plasma wakefields by colliding laser pulses *Nature* **444** 737

[33] Annenkov V V, Volchok E P and Timofeev I V 2016 Generation of high-power electromagnetic radiation by a beam-driven plasma antenna *Plasma Phys. Control. Fusion* **58** 045009

[34] Timofeev I V, Volchok E P and Annenkov V V 2016 Theory of a beam-driven plasma antenna *Phys. Plasmas* **23** 083119

[35] Annenkov V V, Timofeev I V and Volchok E P 2016 Simulations of electromagnetic emissions produced in a thin plasma by a continuously injected electron beam *Phys. Plasmas* **23** 053101

[36] Timofeev I V, Berendeev E A and Dudnikova G I 2017 Simulations of a beam-driven plasma antenna in the regime of plasma transparency *Phys. Plasmas* **24** 093114

[37] Annenkov V V, Berendeev E A, Volchok E P and Timofeev I V 2019 Second harmonic electromagnetic emission in a beam-driven plasma antenna *Plasma Phys. Control. Fusion* **61** 055005

[38] Spitsyn R I, Timofeev I V, Sosedkin A P and Lotov K V 2018 Characterization of wavebreaking time and dissipation of weakly nonlinear wakefields due to ion motion *Phys. Plasmas* **25** 103103

[39] Berenger J 1994 A perfectly matched layer for the absorption of electromagnetic waves *J. Comput. Phys.* **114** 185

[40] Higginson D P, Korneev P *et al* 2019 Laboratory investigation of particle acceleration and magnetic field compression in collisionless colliding fast plasma flows *Commun. Phys.* **2** 60